ISSN 1070-3632, Russian Journal of General Chemistry, 2018, Vol. 88, No. 3, pp. 541–550. © Pleiades Publishing, Ltd., 2018.

Synthesis, Antibacterial and Antileishmanial Activity, Cytotoxicity, and Molecular Docking of New Heteroleptic Copper(I) Complexes with Thiourea Ligands and Triphenylphosphine[1]

A. Saeed[a]*, F. A. Larik[a], F. Jabeen[b], H. Mehfooz[a], S. A. Ghumro[c], H. R. El-Seedi[d], M. Ali[e], P. A. Channar[a], and H. Ashraf[a]**

[a] *Department of Chemistry, Quaid-I-Azam University, Islamabad 45320, Pakistan*
*e-mail: *aamersaeed@yahoo.com; **fayazali@chem.qau.edu.pk*

[b] *Cardiovascular and Metabolic Research Unit, Laurentian University, 935 Ramsey Lake Road, Sudbury, ON P3E 2C6, Canada*

[c] *H.E.J. Research Institute of Chemistry, International Center for Chemical and Biological Sciences, University of Karachi, Karachi 75270, Pakistan*

[d] *Division of Pharmacognosy, Department of Medicinal Chemistry, Uppsala University, Biomedical Center, Box 574, SE-751 23, Uppsala, Sweden*

[e] *Department of Biological Sciences, Quaid-i-Azam University, Islamabad 45320, Pakistan*

Received April 16, 2017

Abstract—A series of copper(I) complexes with triphenylphosphine and *N*-acyl-*N*′-arylthioureas were synthesized and characterized by elemental analysis and IR and NMR (^{1}H, ^{13}C, ^{31}P) spectroscopy. The thiourea ligands and their copper(I) triphenylphosphine complexes were screened for antibacterial and antileishmanial activities and cytotoxicity. The synthesized compounds showed much better activity as compared to glucantime and Kanamycin used as reference drugs. The thiourea ligands showed better activity than their Cu(I) complexes. The molecular docking technique was utilized to ascertain the mechanism of action toward molecular targets (GP63 and 16S-rRNA A-site). It was found that the ligands and complexes were stabilized at the active site by electrostatic and hydrophobic forces, consistent with the corresponding experimental results. The *in silico* study of the binding pattern predicted that one of the synthesized ligands, *N*-(5-chloro-2-nitrophenyl)-*N*′-pentanoylthiourea, can serve as a potential surrogate for hit-to-lead generation and design of novel antibacterial and antileishmanial agents.

Keywords: thiourea, copper(I) complexes, triphenylphosphine, molecular docking, cytotoxicity, anti-leishmanial activity, antibacterial activity

DOI: 10.1134/S1070363218030246

INTRODUCTION

N-Arylthioureas are very good precursors in the synthesis heterocyclic compounds such as imidazolidine-2-thiones, 1,3-thiazoles [1], 1,2,4-thiadiazolidines [2], 1*H*-1,2,4-triazoles [3], tetrazoles [4], 1,2,4-oxathiazoles [5], and 1,3-thiazin-4-ones [6]. Besides having significant importance in the synthetic fields, thioureas possess broad spectrum of biological activities, including antiviral [7], antibacterial [8], antifungal [9], antitubercular [10], herbicidal [11], insecticidal [12], and other pharmacological properties; they act as corrosion inhibitors and antioxidants and are used polymer components [13]. Thiourea derivatives are versatile ligands capable of coordinating to a range of metal centers as neutral molecules, monoanions, or dianions [14–25]. The sulfur, nitrogen, and oxygen donor atoms of thiourea derivatives afford a multitude of bonding possibilities. Both thiourea ligands and their metal complexes exhibit a spacious range of biological activity, including antibacterial, antifungal, antithyroid, antihelmintic, antitubercular, rodenticidal, herbicidal, and plant-growth regulator properties [8, 26–29]. A large number of copper(I) complexes

[1] The text was submitted by the authors in English.

Scheme 1.

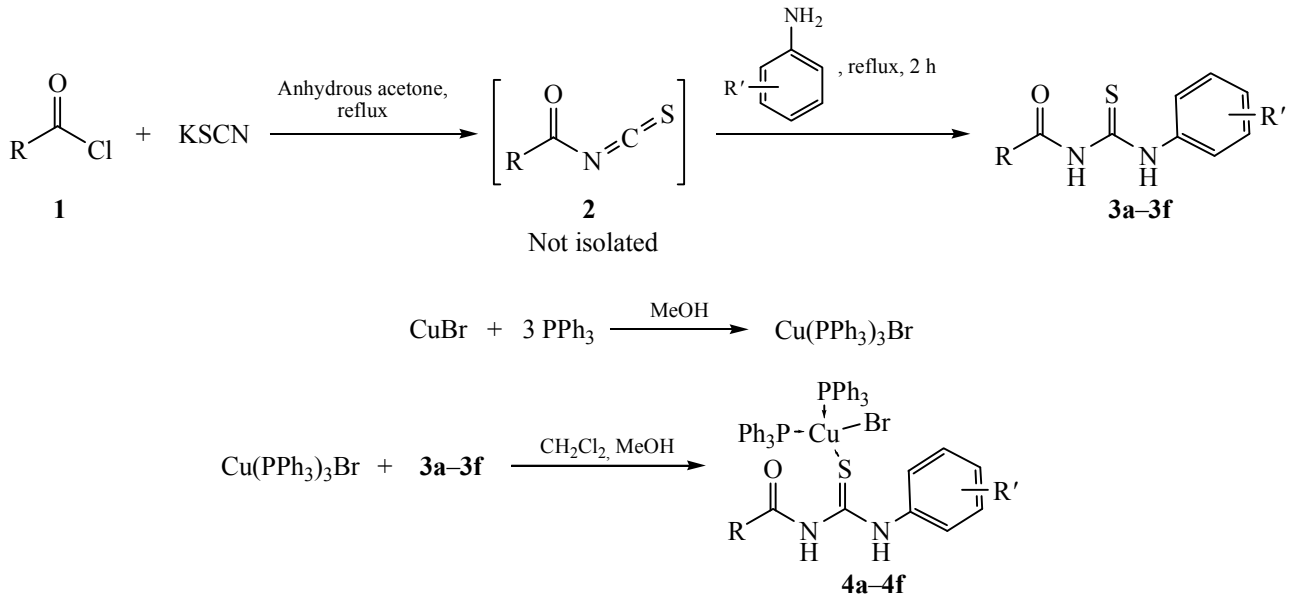

R = C_4H_9, R′ = 2-Br (**a**), 2-Cl-4-O_2N (**b**), 2-O_2N-5-Cl (**c**); R = C_3H_7, R′ = 4-F (**d**), 3-Br (**e**), 2-O_2N-4-Me (**f**).

formed with thiourea and its derivatives relevant in main biological and pharmaceutical areas and involving a variety of structures and compositions have been reported [30–33].

Leishmaniasis is caused by protozoan parasites from the Leishmania genus, and it comprises two major diseases, visceral leishmaniasis (VL) and cutaneous leishmaniasis (CL). While VL is fatal if medically untreated, CL may heal spontaneously or leave disfiguring scars. Leishmaniasis is one of the most ignored tropical diseases and is associated with high morbidity levels. The rate of mortality of VL is approximately 60 000 per year, which is the second highest rate among parasitic diseases, only surpassed by malaria [34–36]. The antileishmanial activity of synthetic and natural compounds has been reviewed comprehensively [37].

Global dissemination of antibacterial resistance has rendered worldwide health practice vulnerable [38]. Antibacterials are highly essential in the prevention and medical treatment of bacterial infection which normally occurs in surgery, organ transplant, cancer chemotherapy, and in veterinary applications [39]. The emergence of methicillin-resistant *Staphylococcus aureus*, penicillin- and vancomycin-resistant enterococci, third-generation cephalosporins-resistant *Escherichia coli*, *Klebsiella pneumoniae*, and *Streptococcus pneumoniae*, extended spectrum β-lactamase, and carbapenem-resistant *Enterobacteriaceae* are most prominent examples that are both widespread and of great concern [40]. A further challenge is that multidrug-resistant bacteria are becoming ubiquitous in both developed and developing countries and that newly discovered antibacterial agents have limited revolutionary mechanisms of action for clinical use [41, 42]. These issues have motivated new strategies and initiatives with the ambition of improving research and development of new antibacterial drugs [43, 44]. Metallopharmaceuticals relate to the use of metal-based species in the treatment of various illnesses and highlight the importance of medicinal inorganic chemistry [45]. Copper complexes of thiourea open new avenues in the antibacterial field.

Herein, we report the synthesis of novel thiourea ligands and their copper(I) complexes with triphenylphosphine and evaluation of their biological properties, in particular cytotoxicity, antileishmanial and antibacterial activity, and multi-target bioactivities. The molecular docking studies were also performed.

RESULTS AND DISCUSSION

Synthesis of thiourea ligands and copper(I) complexes. The thiourea ligands, *N*-acyl-*N*′-arylthioureas **3a**–**3f**, were synthesized starting from two different acid chlorides **1** (butanoyl chloride and pentanoyl chloride) and substituted anilines (Scheme 1). Acid

Table 1. Antileishmanial activity and cytotoxicity of ligands **3a**–**3f** and complexes **4a**–**4f**

Compound no.	IC_{50}, mg/mL (promastigotes)	LD_{50}, mg/mL (human macrophages)	Compound no.	IC_{50}, mg/mL (promastigotes)	LD_{50}, mg/mL (human red blood cells)
3a	4.68	50.0	**4a**	3.125	78.00
3b	1.56	55.5	**4b**	0.780	181.81
3c	0.78	50.0	**4c**	0.390	93.00
3d	48.5	73.0	**4d**	25.000	100.00
3e	43.5	69.0	**4e**	16.600	126.00
3f	17.8	100.0	**4f**	12.500	142.86
Glucantime	6.4	160.0	Glucantime	6.400	160.00

chlorides **1** were treated with an equimolar amount of potassium thiocyanate in acetone to afford the corresponding acyl isothiocyanate intermediates which were not isolated. Condensation of the latter with substituted anilines furnished thiourea derivatives **3a**–**3f** [46]. The IR spectra of **3a**–**3f** showed strong absorption peaks between 3200 and 3400 cm^{-1} which were assigned to N–H stretching vibrations of thiourea [47, 48]. The carbonyl absorption band appeared at about 1700 cm^{-1}, and bands in the region 1600–1500 cm^{-1} indicated the presence of a benzene ring.

Copper(I) bromide was reacted with triphenylphosphine at a ratio of 1 : 3 to obtain the corresponding adduct. The complexation was carried out by reacting tris(triphenylphosphine)copper(I) bromide with ligands **3a**–**3f** in methylene chloride–methanol; the appearance of yellow color indicated the formation of metal complexes **4a**–**4f**. The synthesized ligands and complexes were successfully characterized by spectroscopic techniques.

The ^{1}H NMR spectra of ligands **3a**–**3f** and copper(I) complexes **4a**–**4f** displayed two distinct downfield signals in the region δ 11–13 ppm due to NH protons, the aromatic protons appeared around δ 7–8 ppm, and aliphatic protons resonated at δ ~2–3 ppm. In the ^{13}C NMR spectra of **3a**–**3f** and **4a**–**4f**, characteristic peaks appeared at δ_C 180 ppm due to C=S carbon atom, and the carbonyl carbon signal was located at δ_C 170–175 ppm. Aromatic carbon signals were observed in the region δ_C 140–120 ppm. sp^3-Carbons resonated around δ_C 30–15 ppm. Some difference in the positions of the C=S signal was observed in the ^{13}C NMR spectra of the ligands and the corresponding complexes. The ^{31}P NMR spectra of the complexes contained a signal at δ_P –6.0 ppm due to the presence of triphenylphosphine ligands.

Antileishmanial activity and cytotoxicity. Compound **3c** showed excellent antileishmanial activity in the series of thiourea ligands while compound **3d** showed poor activity (Table 1). Copper(I) complexes **4c** and **4b** showed excellent activity while **4e** showed least activity in the series of complexes. Furthermore, the copper(I) complexes were more active than the corresponding thiourea ligands. All these compounds were characterized by high toxicity at high concentration, and they showed less toxicity at lowest concentration; therefore, they can be useful as pharmaceuticals at low doses as they show very low toxicity for human healthy cells.

Antibacterial activity. The ligands and the complexes were evaluated for their potential antibacterial activity against four bacterial strains. The antibacterial activity was determined by the agar diffusion method by measuring the diameter of zones showing complete inhibition (mm) with reference to positive control (Kanamycin). Experiments were performed in triplicates, and the results are summarized in Table 2. Two compounds, **3c** and **3d**, showed good antibacterial activity against both gram positive and gram negative bacterial strains. Compounds **3a**, **3b**, and **3f** exhibited minimum antibacterial activity against all four bacterial strains. Except for compound **3c**, the thiourea ligands were generally less active than their copper(I) complexes. The copper complexes showed moderate activity against all four bacterial strains, the most potent being compound **4c**.

Molecular docking study. MOE (Molecular Operating Environment) is an interactive molecular

Table 2. Antibacterial activity of ligands **3a**–**3f** and complexes **4a**–**4f**

Compound no.	Inhibition zone (mm) at 200 μg/mL			
	Micrococcus luteus	*Staphylococcus aureus*	*Escherichia coli*	*Enterobacter aerogenes*
3a	12	10	10	6
3b	0	12	5	0
3c	33	35	30	32
3d	13	14	12	7
3e	14	15	10	8
3f	7	6	6	5
4a	17	18	18	19
4b	30	31	15	15
4c	28	33	17	27
4d	25	28	15	25
4e	27	30	15	0
4f	31	25	27	22
Kanamycin	32	34	28	24

graphics program for computing and displaying feasible docking modes of various targets, which was used to carry out current *in silico* studies of the binding modes of the thiourea ligands and their copper(I) complexes to the leishmanolysin GP63 active site and *E. coli* 16S-rRNA A-site (PDB code 1j7t). The parameters and charges were assigned with MMFF94x force field. For further studies, we selected variants with the minimal energy of the receptor–inhibitor complex, achieved as a result of the docking simulations. The active sites in both targets were found to be a wide cleft lined with both hydrophilic and hydrophobic amino acids. All docked compounds were represented in balls and sticks to clarify the preferred binding mode of compounds in the target crystal structures shown in Fig. 1.

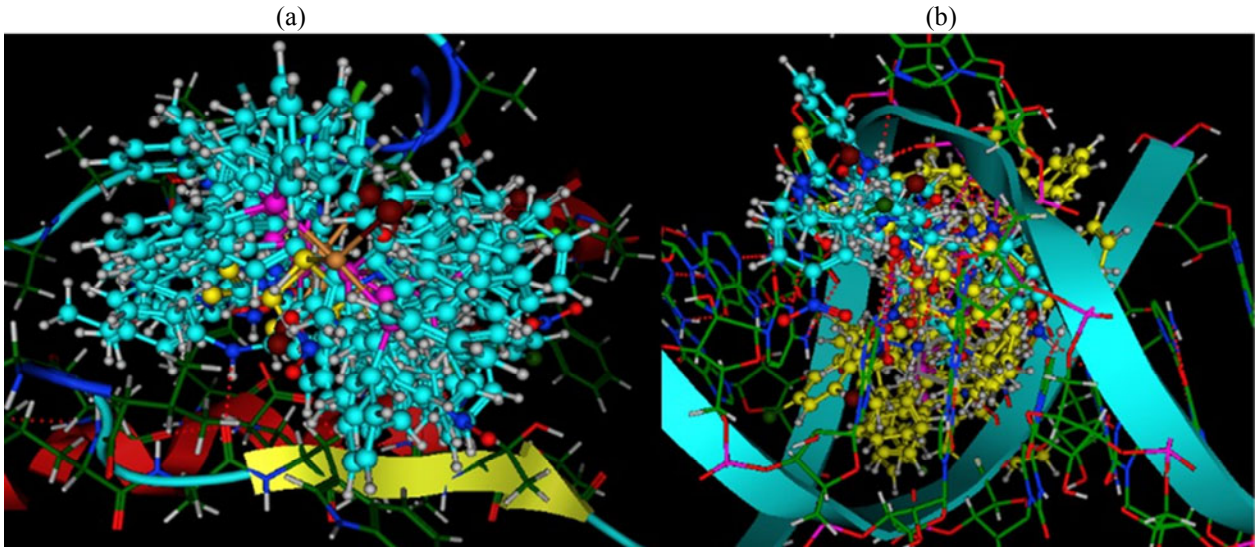

Fig. 1. (a) Superimpositions of the most favorable docked conformations of the ligands inside the active site of GP63 (PDB ID: ILM); receptor is shown as cartoons and ribbons (red, yellow); (b) superimposition of minimum-energy docked conformations inside the active site of 1j7t. Ligands are shown in ball and stick mode in cyan color, complexes **4a** to **4d** are shown in yellow ball and stick mode; the key residues are presented in stick mode (green); backbone is shown in cyan colored ribbon.

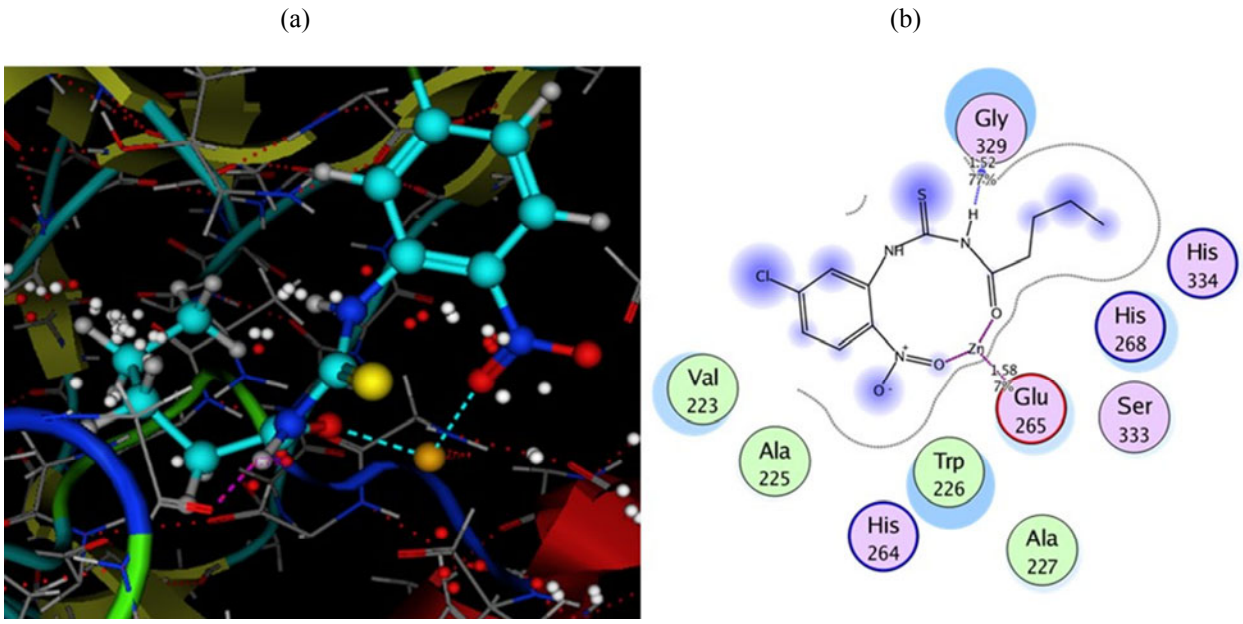

Fig. 2. Docking pose of **3c** inside the active site of GP63: (a) docking pose of **3c** in 3D space. Molecule **3c** is shown in stick mode (cyan color), the receptor is shown in yellow colored cartoons and ribbons, and the key residues are shown in green color stick mode; H-bonds of the ligand atoms are shown in purple colored dashed lines; the interaction with Zn is shown in cyan colored dashed lines; (b) interaction of **3c** with GP63 in 2D space.

The highly favorable conformations of ligands **3a**, and **3c**–**3f** are anchored inside the active site cleft through hydrogen bonding with Gly329, while complexes **4a**, **4b**, **4d**, and **4e** form strong hydrogen bonds with the key residues such as Pro347, Trp22, Ala 225, and Gly329, respectively. Few hydrophobic interactions of the ligands are also observed with Val223, Val261, Ala227, Trp226, and Ala328 in addition to strong electrostatic interactions with Glu268, Gly329, His268, Ser333, Thr228, Glu220, and Glu221.

Another characteristic feature that discriminates the binding mode of these compounds is that the zinc ion present in the active site is chelated by the ligand and Glu265. In the case of ligands **3c** and **3f**, the zinc atom is involved in close contact with oxygen atoms of the carbonyl and nitro groups to form a very stable 10-membered ring which is further stabilized by two strong hydrogen bonds with Gly329 and Glu265, as well as by hydrophobic and polar interactions. Figure 2 depicts the preferred docked orientation of ligand **3c** in the binding cavity of the protein.

The optimized geometries of the ligands and complexes were docked to the active site of the minimized eubacterial ribosomal decoding A site (*E. coli* 16S rRNA A-site). Ligands **3a** to **3f** formed one cluster, and all the respective metal complexes formed another cluster (Fig. 1b). All thiourea ligands and complexes bound tightly into the major grove of RNA strand. Nitrogen bases A15, A17, A29, C25, C28, G12, G13, G15, G18, G26, U14, and U27 were found to be important for activities of antibacterial compounds. The phosphorus atom present in the copper(I) complexes proved to stabilize them in the active site by establishing contacts with bases G13, G26, and U27. All complexes except **4c** were anchored in the active site through P–nitrogen base interactions in addition to hydrogen bonding. The carbonyl oxygen of **3a**, **3c**, **4a**, **4b**, **4d**, and **4f** formed strong hydrogen bonds with some key nitrogen bases such as A17, A29, and U27.

Ligand **3c** was stabilized in the binding pocket by forming two strong hydrogen bonds with A17 and A29 bases in addition to numerous electrostatic contacts with A17, G15, A29, C28, G26, U14, and U27. Copper(I) complexes **4a**–**4f** were stabilized in the binding pocket by arranging phenyl rings in coplanar position. Figure 3 represents the binding pattern of ligand **3c** inside the major groove of the duplex.

In summary, novel thiourea ligands and their copper(I) triphenylphosphine complexes were synthesized and evaluated for antibacterial and antileishmanial activity and cytotoxicity. The synthesized

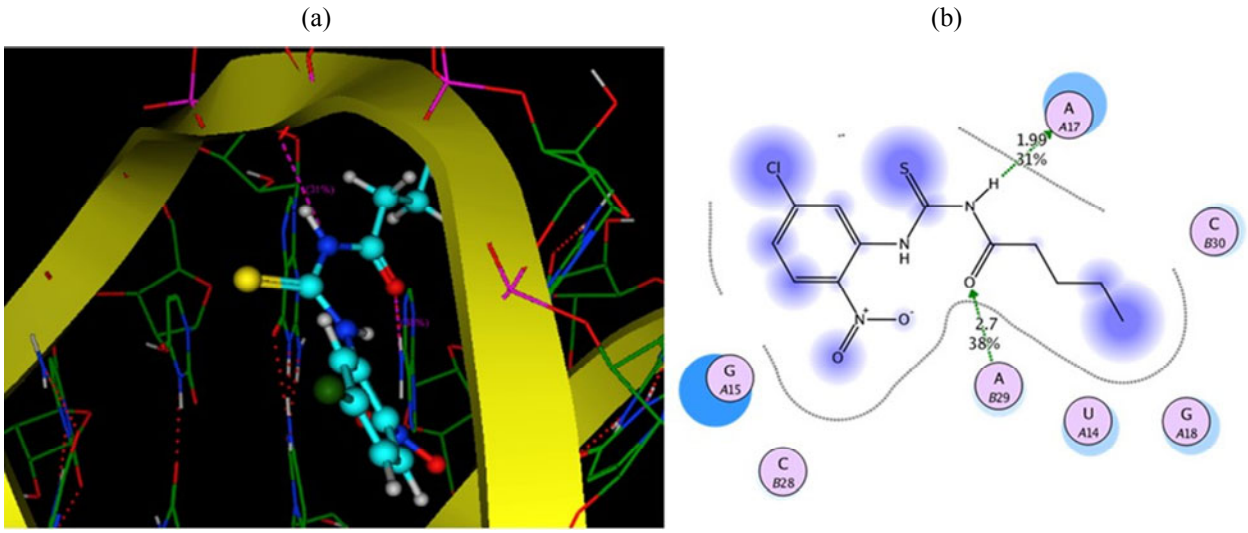

Fig. 3. Molecular docking analysis. (a, b) Docking pose of **3c** in 3D space. Molecule **3c** is shown in stick mode (cyan color), receptor is shown in yellow colored cartoons and ribbons, and key residues are shown in green color stick mode. (a) H-bonding of ligand atoms with Val300, Trp22, Trp114, Ile261, and Ile299 shown in green colored solid line; (b) π–H interaction of ligand **3c** with Val300, Ala219, Arg218, and Ile261, represented in solid green lines.

compounds possess excellent potential against bacterial and *Leishmania* species. The copper complexes showed better activity than the corresponding thiourea ligands. Molecular docking computations revealed good binding mode of the ligands and complexes to biological targets through electrostatic and hydrophobic interactions. Compound **3c** can serve as the potential candidate for hit-to-lead generation and design of novel antibacterial and antileishmanial agents.

EXPERIMENTAL

The melting points were measured in open capillaries with a Thomas Hoover Unimelt apparatus and are uncorrected. All reagents and solvents were purchased from Sigma Aldrich, Fluka, and E. Merck. Acetone (99.9% pure) and *n*-hexane (95%) were purified, dried, and distilled according to reported methods before use. Potassium thiocyanate (98%), acid chlorides (99%), and substituted anilines were used without further purification. The purity of the isolated compounds was checked by TLC on silica gel G plates using petroleum ether–ethyl acetate (7 : 3, v/v) as eluent; spots were visualized using a UV lamp. The FTIR spectra were recorded on a Bio-Rad Excalibur FTS 3000 MX spectrophotometer. The NMR spectra were recorded in DMSO-d_6 on a Bruker spectrometer (300 MHZ for ^{1}H and 75 MHz for ^{13}C) using tetramethylsilane as standard.

General procedure for the synthesis of ligands 3a–3f. Pentanoyl or butanoyl chloride was added to a solution of potassium thiocyanate in anhydrous acetone, and the mixture was stirred for about 1.5 h. The corresponding aniline was then added, and the mixture was refluxed for ~2 h.

General procedure for the synthesis of complexes 4a–4f. Copper(I) bromide was treated with 3 equiv of triphenylphosphine in methanol. The mixture was stirred for 4–5 h, and the pale yellow solid was filtered off and dried. Yield of $Cu(PPh_3)_3Br$ 90%. A solution of thiourea **3a–3f** in 10 mL of methylene chloride were mixed with a solution of an equimolar amount of $Cu(PPh_3)_3Br$ in 10 mL of methanol, and the mixture was stirred for 5–6 h. The formation of yellow solution indicated completion of the reaction. The solvent was evaporated to obtain complexes **4a–4f** as yellow solids.

***N*-[(2-Bromophenyl)carbamothioyl]pentanamide (3a).** Yield 98%, yellow crystalline solid, mp 215°C, R_f 0.61 (*n*-hexane–EtOAc, 1 : 1). IR spectrum, ν, cm^{-1}: 3199 (N–H), 2984 (C–H_{arom}) 1686 (C=O), 1510 (C=C_{arom}), 1420 (δ C–H), 1299 (C=S). ^{1}H NMR spectrum, δ, ppm: 12.80 s (1H, NH), 11.88 s (1H, NH), 8.12 d (1H, J = 7.8 Hz), 7.83 d.d (1H, J = 7.2, 4.5 Hz), 7.53 d.d (1H, J = 7.6, 4.2 Hz), 7.47 d (1H, J = 7.8 Hz), 2.4 t (2H), 2.0 quint (2H), 1.8 sext (2H), 1.5 t (3H). ^{13}C NMR spectrum, δ_C, ppm: 189.1 (C=S), 170.5 (C=O), 146.4, 139.2, 136.7, 132.2, 129.2, 127.6 (C_{arom}), 40, 24, 20, 16 (CH_3). Found, %: C 45.59; H 4.89; N 8.79. $C_{12}H_{15}BrN_2OS$. Calculated, %: C 45.73; H 4.80; N 8.89.

***N*-[(2-Chloro-4-nitrophenyl)carbamothioyl]pentanamide (3b).** Yield 89%, yellow crystalline solid, mp 205°C, R_f 0.68 (*n*-hexane–EtOAc, 1 : 1). IR spectrum, ν, cm^{-1}: 3185 (N–H), 2996 (C–H_{arom}), 1685 (C=O), 1575 (NO_2), 1509 (C=C_{arom}), 1417 (δ C–H), 1345 (NO_2), 1259 (C=S). ^{1}H NMR spectrum, δ, ppm: 11.61 s (1H, NH), 11.41 s (1H, NH), 8.31 d (1H, *J* = 3.9 Hz), 7.83 d (1H, *J* = 7.9 Hz), 7.53 d (1H, *J* = 6.5 Hz), 2.43 t (2H), 2.12 quint (2H), 1.83 sext (2H), 1.54 t (3H). ^{13}C NMR spectrum, δ_C, ppm: 182.4 (C=S), 175.6 (C=O), 140.9, 137.1, 135.1, 131.5, 127.7, 125.5 (C_{arom}), 40, 22, 18, 14. Found, %: C 45.53; H 4.49; N 13.79. $C_{12}H_{14}ClN_3O_3S$. Calculated, %: C 45.67; H 4.60; N 13.89.

***N*-[(5-Chloro-2-nitrophenyl)carbamothioyl]pentanamide (3c).** Yield 89%, white crystalline solid, mp 190°C, R_f 0.68 (*n*-hexane–EtOAc, 1 : 1). IR spectrum, ν, cm^{-1}: 3181 (N–H), 2986 (C–H_{arom}), 1691 (C=O), 1570 (NO_2), 1512 (C=C_{arom}), 1419 (δ C–H), 1349 (NO_2), 1259 (C=S). ^{1}H NMR spectrum, δ, ppm: 11.71 s (1H, NH), 11.51 s (1H, NH), 8.21 d (1H, *J* = 3.7 Hz), 7.80 d (1H, *J* = 6.9 Hz), 7.48 d (1H, *J* = 5.5 Hz), 2.51 t (2H), 2.24 quint (2H), 1.97 sext (2H), 1.57 t (3H). ^{13}C NMR spectrum, δ_C, ppm: 181.8 (C=S), 176.7 (C=O), 142.9, 136.1, 134.1, 132.5, 128.7, 124.4 (C_{arom}), 40, 25, 20, 17. Found, %: C 45.55; H 4.51; N 13.81. $C_{12}H_{14}ClN_3O_3S$. Calculated, %: C 45.67; H 4.60; N 13.89.

***N*-[(4-Fluorophenyl)carbamothioyl]butanamide (3d).** Yield 95%, light yellow solid, mp 181°C, R_f 0.58 (*n*-hexane–EtOAc, 1 : 1). IR spectrum, ν, cm^{-1}: 3186 (N–H), 2994 (C–H_{arom}), 1687 (C=O), 1571 (NO_2), 1507 (C=C_{arom}), 1415 (δ C–H), 1338 (NO_2), 1295 (C=S). ^{1}H NMR spectrum, δ, ppm: 11.77 s (1H, NH), 11.55 s (1H, NH), 7.73 d (2H, H_{arom}, *J* = 7.8 Hz), 7.47 d (2H, H_{arom}, *J* = 7.8 Hz), 2.3 t (2H), 1.9 sext (2H), 1.4 t (3H). ^{13}C NMR spectrum, δ_C, ppm: 187.1 (C=S), 170.1 (C=O), 134.1, 132.5, 128.7, 126.5 (C_{arom}), 33, 23, 18. Found, %: C 54.52; H 5.52; N 12.80. $C_{11}H_{13}FN_2OS$. Calculated, %: C 54.67; H 5.60; N 12.89.

***N*-[(3-Bromophenyl)carbamothioyl]butanamide (3e).** Yield 98%, yellow crystalline solid, mp 202°C, R_f 0.61 (*n*-hexane–EtOAc, 1 : 1). IR spectrum, ν, cm^{-1}: 3199 (N–H), 2984 (C–H_{arom}), 1685 (C=O), 1509 (C=C), 1419 (δ C–H), 1299 (C=S). ^{1}H NMR spectrum, δ, ppm: 12.80 s (1H, NH), 11.88 s (1H, NH), 7.89–7.32 m (4H, H_{arom}), 2.4 t (2H), 1.8 sext (2H), 1.5 t (3H, *J* = 3.5 Hz). ^{13}C NMR spectrum, δ_C, ppm: 189.1 (C=S), 170.5 (C=O), 146.4, 139.2, 136.7, 132.2, 129.2, 127.6 (C_{arom}), 35, 24, 16 (CH_3). Found, %: C 43.53; H 4.29; N 9.23. $C_{11}H_{13}BrN_2OS$. Calculated, %: C 43.86; H 4.35; N 9.30.

***N*-[(4-Methyl-2-nitrophenyl)carbamothioyl]butanamide (3f).** Yield 89%, yellow crystalline solid, mp 255°C, R_f 0.68 (*n*-hexane–EtOAc, 1 : 1). IR spectrum, ν, cm^{-1}: 3185 (N–H), 2996 (C–H_{arom}), 1685 (C=O), 1575 (NO_2), 1509 (C=C_{arom}), 1417 (δ C–H), 1345 (NO_2), 1259 (C=S). ^{1}H NMR spectrum, δ, ppm: 11.61 s (1H, NH), 11.41 s (1H, NH), 7.35–6.9 m (3H, H_{arom}), 2.51 s (3H), 2.4 t (2H, *J* = 2.7 Hz), 1.3 sext (2H), 0.9 t (3H, *J* = 4.1 Hz). ^{13}C NMR spectrum, δ_C, ppm: 182 (C=S), 175.6 (C=O), 140.9, 137.1, 135.1, 131.5, 127.7, 125.5 (C_{arom}), 37, 30, 24, 17 (CH_3). Found, %: C 51.16; H 5.27; N 14.18. $C_{12}H_{15}N_3O_3S$. Calculated, %: C 51.25; H 5.38; N 14.95.

{*N*-[(2-Bromophenyl)carbamothioyl]pentanamide}-[bis(triphenylphosphine)]copper(I) bromide (4a). Yield 75%, yellow crystalline solid, mp 179–181°C, R_f 0.61 (*n*-hexane–EtOAc, 1 : 1). ^{1}H NMR spectrum, δ_C, ppm: 12.80 s (1H, NH), 11.88 s (1H, NH), 8.12 d (1H, *J* = 7.8 Hz), 7.83 d.d (1H, *J* = 7.2, 4.5 Hz), 7.53 d.d (1H, *J* = 7.6, 4.2 Hz), 7.47 d (1H, *J* = 7.8 Hz), 7.4–7.09 (30H, Ph), 2.4 t (2H), 2.0 quint (2H), 1.8 sext (2H), 1.5 t (3H, *J* = 4.2 Hz). ^{13}C NMR spectrum, δ_C, ppm: 179.1 (C=S), 177.5 (C=O), 134.4, 133.8, 133.46, 133.2, 126.72, 125.6 (C_{arom}), 133.1, 129.58, 128.5, 128.08 (Ph), 37, 26, 22, 14. Found, %: C 58.17; H 4.64; N 2.84. $C_{48}H_{45}Br_2CuN_2OP_2S$. Calculated, %: C 58.01; H 4.48; N 2.97.

{*N*-[(2-Chloro-4-nitrophenyl)carbamothioyl]pentanamide}[bis(triphenylphosphine)]copper(I) bromide (4b). Yield 77%, yellow crystalline solid, mp 173°C, R_f 0.68 (*n*-hexane–EtOAc, 1 : 1). ^{1}H NMR spectrum, δ, ppm: 12.58 s (1H, NH), 11.85 s (1H, NH), 8.19 d (1H, *J* = 3.9 Hz), 8.18 d (1H, *J* = 7.9 Hz), 7.86 d (1H, *J* = 6.5 Hz), 7.44–7.28 m (30H, Ph), 2.5 t (2H, *J* = 3.2 Hz), 1.58 quint (2H), 1.38 sext (2H), 0.93 t (3H, *J* = 3.4 Hz). ^{13}C NMR spectrum, δ_C, ppm: 180.8 (C=S), 175.6 (C=O), 144.9, 134.1, 130.1, 129.5, 128.7, 125.5 (C_{arom}), 133.61, 133.25, 132.16, 131.43 (Ph) 40, 26, 22, 14. Found, %: C 59.16; H 4.27; N 4.25. $C_{47}H_{42}BrClCuN_3O_3P_2S$. Calculated, %: C 59.23; H 4.38; N 4.35.

{*N*-[(5-Chloro-2-nitrophenyl)carbamothioyl]pentanamide}[bis(triphenylphosphine)]copper(I) bromide (4c). Yield 79%, white crystalline solid, mp 195°C, R_f 0.68 (*n*-hexane–EtOAc, 1 : 1). ^{1}H NMR spectrum, δ, ppm: 12.96 s (1H, NH), 12.41 s (1H, NH), 9.12 d (1H, *J* = 3.7 Hz), 9.1 d (1H, *J* = 6.9 Hz), 8.064 d (1H, *J* = 5.5 Hz), 2.64 t (2H), 1.72 quint (2H), 1.48 sext (2H), 1.36 t (3H, *J* = 2.8 Hz). ^{13}C NMR spectrum, δ_C, ppm:

181.8 (C=S), 176.7 (C=O), 135.56, 134.9, 134.2, 128.5, 121.7, 120.98 (C_{arom}), 134, 133.44, 130.28, 128.93 (Ph), 37, 26, 22, 14. Found, %: C 59.12; H 4.26; N 4.23. $C_{48}H_{46}BrClCuN_3O_3P_2S$. Calculated, %: C 58.23; H 4.38; N 4.35.

{*N*-[(4-Fluorophenyl)carbamothioyl]butanamide}-[bis(triphenylphosphine)]copper(I) bromide (4d). Yield 85%, light yellow solid, mp 165°C, R_f 0.58 (*n*-hexane–EtOAc, 1 : 1). ^{1}H NMR spectrum, δ, ppm: 12.8 s (1H, NH), 11.82 s (1H, NH), 8.27 d (2H, H_{arom}, J = 7.8 Hz), 7.97 d (2H, H_{arom}, J = 7.8 Hz), 7.42–7.26 m (30H, Ph), 2.5 t (2H), 1.65 sext (2H), 0.94 t (3H). ^{13}C NMR spectrum, δ_C, ppm: 179.25 (C=S), 175.86 (C=O), 144.95, 144.06, 124.73, 124.78 (C_{arom}), 134, 133.44, 130.28, 128.93 (Ph), 38, 18, 13.9. Found, %: C 62.12; H 4.82; N 2.91. $C_{47}H_{43}BrCuFN_2OP_2S$. Calculated, %: C 62.25; H 4.98; N 3.05.

{*N*-[(3-Bromophenyl)carbamothioyl]butanamide}-[bis(triphenylphosphine)]copper(I) bromide (4e). Yield 83%, yellow crystalline solid, mp 161°C, R_f 0.61 (*n*-hexane–EtOAc, 1 : 1). ^{1}H NMR spectrum, δ, ppm: 12.80 s (1H, NH), 11.88 s (1H, NH), 8.67–7.9 m (4H, H_{arom}), 7.6–7.2 (30H, Ph), 2.4 t (2H, J = 2.7 Hz), 1.8 sext (2H), 1.5 t (3H, J = 2.5 Hz). ^{13}C NMR spectrum, δ_C, ppm: 179.1 (C=S), 175.5 (C=O), 147.9, 139.2, 136.7, 134.2, 121.2, 119.6 (C_{arom}), 134, 133.44, 130.28, 128.93 (Ph), 38, 19, 13. Found, %: C 58.15; H 4.45; N 3.07. $C_{47}H_{43}Br_2CuN_2OP_2S$. Calculated, %: C 58.25; H 4.57; N 2.99.

{*N*-[(4-Methyl-2-nitrophenyl)carbamothioyl]-butanamide}[bis(triphenylphosphine)]copper(I) bromide (4f). Yield 78%, yellow crystalline solid, mp 151°C, R_f 0.68 (*n*-hexane–EtOAc, 1 : 1). ^{1}H NMR spectrum, δ, ppm: 12.51 s (1H, NH), 11.66 s (1H, NH), 8.25–8.06 m (3H, H_{arom}), 7.42–7.26 (30H, Ph), 2.51 s (3H), 2.4 t (2H, J = 3.2 Hz), 1.3 sext (2H), 0.9 t (3H, J = 3.1Hz). ^{13}C NMR spectrum, δ_C, ppm: 179.89 (C=S), 176.02 (C=O), 145.9, 140.1, 135.1, 134.5, 125.7, 121.5 (C_{arom}), 134, 133.44, 130.28, 128.93 (Ph), 38, 31, 24, 14. Found, %: C 60.64; H 4.67; N 4.34. $C_{48}H_{45}BrCuN_3O_3P_2S$. Calculated, %: C 60.73; H 4.79; N 4.45.

Antileishmanial activity assay. Stock solutions of the ligands and complexes were prepared by dissolving 1 mg of a substance in 1 mL of DMSO. *Leishmania tropica* KWH23 promastigotes were grown in M199 (Medium 199) with streptomycin and 25 mM HEPES buffer [4-(2-hydroxyethyl)piperazine-1-ethanesulfonic acid] supplemented with 10% heat-inactivated FBS (fetal bovine serum) at pH 7.2 and were maintained at 24°C. Medium 199 containing promastigote culture was dispersed in the wells of a 96-well microtiter plate to yield 2×10^6 cells per milliliter in each well. Next the ligands and complexes were added serially to each well of the plate, and 2 wells were left for the positive and negative controls. DMSO was taken as the negative control and successively diluted in the M199 medium. Glucantime was used as the positive control (IC_{50} 6.4 μg/mL) and was incubated overnight in the dark at 25°C for 72 h. The number of viable cells was counted with a Neubauer chamber under a microscope (Micros, Austria). All *in vitro* experiments were run in triplicate, and the results were expressed as inhibition percent in cell number. The drug concentration required for 50% inhibition (IC_{50}) was determined using SPSS 22 software.

Cytotoxicity/hemolysis assays. Fresh human red blood cells were washed with phosphate-buffered saline (PBS) for three times; 100 μL of red blood cell suspension in PBS was placed in each well of 96-well plates, and 100 μL of PBS was added to each well. The plates were incubated for 1 h at 37°C. The cell suspensions were taken out and centrifuged at 1000 g for 5 min. Aliquots of supernatant were transferred to 96-well plates and hemoglobin release was monitored at λ 576 nm using a microplate reader. A red blood cell suspension in PBS was used as negative control. The absorbance of wells with red blood cells lysed with 0.5% Triton X-100 was taken as 100% hemolysis. The percentage of hemolysis was calculated using the formula Hemolysis (%) = [(D_{576} in the nanoparticle solution – D_{576} in PBS)/(D_{576} in 0.5% Triton X-100 – D_{576} in PBS)] × 100, where D_{576} is the optical density at λ 576 nm.

Antibacterial assay. Two gram positive (*Staphylococcus aureus* ATCC 6538 and *Micrococcus luteus* ATCC 10 240) and two gram negative (*Escherichia coli* ATCC 15224) and *Enterobacter aerogenes* ATCC 13 048) were cultured in nutrient broth for 24 h at 37°C. These cultured strains were used as inoculum (1%) to run the assay. Each bacterial strain was added to nutrient agar medium at 45°C, poured into sterile Petri dishes and allowed to solidify. A solution of a test compound (5 μL) with a concentration of 200 μg/mL was poured on sterile filter paper discs (4 mm) and placed on nutrient ager plates. Kanamycin and DMSO were used as positive and negative controls, respectively, on each plate. The assay was performed in triplicate, and plates were

incubated at 37°C for 24–48 h. The antibacterial activity was determined by measuring the diameter of zones showing complete inhibition (mm) with the help of a vernier caliper.

Molecular docking study. Building module of the Molecular Operating Environment (MOE-2014) program was used to prepare the ligand files for the molecular docking studies [49]. The geometries of each compound were drawn in building panel of MOE and subjected to energy optimization at a standard MMFF94 force field level with a 0.0001 kcal/mol energy gradient convergence criterion [50]. The energy minimized 3D geometries were saved in a molecular data base (mdb) file for further studies.

The receptor preparation steps involve 3D protonation, energy minimization followed by active site identification [51]. The crystal structures of GP63 [52, 53] and 1j7t [54] were downloaded from the protein data bank. GP63 was devoid of cognate ligand while 1ijt7 was complexed with the cognate ligand. The complexes were imported to MOE, where structures were edited by removing solvents and all water molecules. The structure preparation module of MOE was used for 3D protonation of receptors, followed by energy minimization using default parameters. LigX module of the MOE was used to identify the active site in 1j7t, which was marked around the co-crystallized ligand. Since the GP63 was devoid of cognate ligand so active site was identified by using site finder module of the software. The alpha center was created, followed by creation of dummy atoms in the active site.

The optimized ligands were docked with the RNA and GP63 (PDB codes 1j7t and ILM, respectively) using the MOE-Dock module. Total of 30 independent docking computations were performed using the MOE docking simulation program. The docked conformations were analyzed and the best-scored conformation for each ligand was chosen for detailed studies of interaction evaluation. The 2-dimensional ligand–protein interactions were visualized by analyzing the ligand–protein complex of the lowest-energy docking pose by using the MOE ligand interactions program.

REFERENCES

1. Kodomari, M., Suzuki, M., Tanigawa, K., and Aoyama, T., *Tetrahedron Lett*., 2005, vol. 46, p. 5841. doi 10.1016/j.tetlet.2005.06.135
2. Batey, R.A. and Powell, D.A., *Org Lett*., 2000, vol. 2, p. 3237. doi 10.1021/ol006465b
3. Larik, F.A., Saeed, A., Channar, P.A., Ismail, H., Dilshad, E., and Mirza, B., *Bangladesh J. Pharmacol*., 2016, vol. 11, p. 894. doi 10.3329/bjp.v11i4.29059
4. Hartmann, H., Liebscher, J., and Czerney, P., *Tetrahedron*, 1985, vol. 41, p. 5371. doi 10.1016/S0040-4020(01)96792-4
5. Cunha, S., Rodrigues, M.T., de Silva, C.C., Jr,, Napolitano, H.B., Vencato, I., and Lariucci, C., *Tetrahedron*, 2005, vol. 61, p. 10 536. doi 10.1016/j.tet.2005.08.052
6. Saeed, A., Flörke, U., and Erben, M.F., *J. Sulfur Chem*., 2014, vol. 35, p. 318. doi 10.1080/17415993.2013.834904
7. Larik, F.A., Saeed, A., Channar, P.A., Muqadar, U., Abbas, Q., Hassan, M., Seo, S.Y., and Bolte, M., *Eur. J. Med. Chem*., 2017, vol. 141, p. 273. doi 10.1016/j.ejmech.2017.09.059
8. Eweis, M., Elkholy, S.S., and Elsabee, M.Z., *Int. J. Biol. Macromol*., 2006, vol. 38, p. 1. doi 10.1016/j.ijbiomac.2005.12.009
9. Sriram, D., Yogeeswari, P., Dinakaran, M., and Thirumurugan, R., *J. Antimicrob. Chemother*., 2007, vol. 59, p. 1194. doi 10.1093/jac/dkm085
10. Saeed, A., Shah, M.S., Larik, F.A., Khan, S.U., Channar, P.A., Flörke, U., and Iqbal, J., *Med. Chem. Res*., 2017, vol. 26, p. 1635. doi 10.1007/s00044-017-1829-6
11. Saeed, A., Channar, P.A., Larik, F.A., Jabeen, F., Muqadar, U., Saeed, S., Flörke, U., Ismail, H., Dilshad, E., and Mirza, B., *Inorg. Chim. Acta*, 2017, vol. 464, p. 204. doi 10.1016/j.ica.2017.05.036
12. Saeed, A., Sajid, R., Channar, P.A., Larik, F.A., Qamar, A., Hassan, M., Raza, H., and Seo, S.-Y., *Drug Res. (Stuttgart)*, 2017, vol. 67, no. 10, p. 596. doi 10.1055/s-0043-113832
13. Arslan, H., Duran, N., Borekci, G., Koray, O.C., and Akbay, C., *Molecules*, 2009, vol. 14, p. 519. doi 10.3390/molecules14010519
14. Park, Y., Harper, K.C., Kuhl, N., Kwan, E.E., Liu, R.Y., and Jacobsen, E.N., *Science*, 2017, vol. 355, p. 162. doi 10.1126/science.aal1875
15. Arjunan, V., Anitha, R., Durgadevi, G., Marchewka, M.K., and Mohan, S., *J. Mol. Struct*., 2017, vol. 1133, p. 187. doi 10.1016/j.molstruc.2016.12.011
16. Binzet, G., Arslan, H., Florke, U., Kulcu, N., and Duran, N., *J. Coord. Chem*., 2006, vol. 59, p. 1395. doi 10.1080/00958970500512633
17. Ugur, D., Arslan, H., and Kulcu, N., *Russ. J. Coord. Chem*., 2006, vol. 32, p. 669. doi 10.1134/S1070328406090089
18. Channar, P.A., Saeed, A., Larik, F.A., Rashid, S., Iqbal, Q., Rozi, M., Younis, S., and Mahar, J., *Biomed. Pharmacother*., 2017, vol. 94, p. 499. doi 10.1016/j.biopha.2017.07.139
19. Saeed, A., Mahesar, P.A., Channar, P.A., Larik, F.A., Abbas, Q., Hassan, M., Raza, H., and Seo, S.Y., *Chem. Biodiversity*, 2017, vol. 14, article ID e1700035. doi 10.1002/cbdv.201700035

20. Henderson, W., Nicholson, B.K., Dinger, M.B., and Bennett, R.L., *Inorg. Chim. Acta*, 2002, vol. 338, p. 218. doi 10.1016/S0020-1693(02)01017-4
21. Ferreira, M., Assunção, L.S., Silva, A.H., Filippin-Monteiro, F.B., Creczynski-Pasa, T.B., and Sá, M.M., *Eur. J. Med. Chem*., 2017, vol. 129, p. 151. doi. 10.1016/j.ejmech.2017.02.013
22. Ozturk, I.I., Yarar, S., Banti, C.N., Kourkoumelis, N., Chrysouli, M.P., Manoli, M., Tasiopoulos, A.J., and Hadjikakou, S.K., *Polyhedron*, 2017, vol. 123, p. 152. doi 10.1016/j.poly.2016.11.008
23. Zuckerman, R.L. and Bergman, R.G., *Organometallics*, 2000, vol. 19, p. 4795. doi 10.1021/om000614c
24. Channar, P.A., Saeed, A., Albericio, F., Larik, F.A., Abbas, Q., Hassan, M., Raza, H., and Seo, S.Y., *Molecules*, 2017, vol. 22, p. 1352. doi 10.3390/molecules22081352
25. Yuan, Y.F., Wang, J.T., Gimeno, M.C., Laguna, A., and Jones, P.G., *Inorg. Chim. Acta*, 2001, vol. 324, p. 309. doi 10.1016/S0020-1693(01)00661-2
26. Zhang, Y.M., Wei, T.B., Xian, L., and Gao, L.M., *Phosphorus, Sulfur Silicon Relat. Elem*., 2004, vol. 179, p. 2007. doi 10.1080/10426500490473456
27. Goncalves, I.L., de Azambuja, G.O., Kawano, D.F. and Eifler-Lima, V.L., *Mini-Rev. Org. Chem*., 2018, vol. 15, p. 28. doi 10.2174/1570193X14666170518125219
28. Saeed, A., Channar, P.A., Larik, F.A., and Flörke, U., *Synlett*, 2016, vol. 27, p. 1371. doi 10.1055/s-0035-1561848
29. Saeed, A., Mahesar, P.A., Channar, P.A., Abbas, Q., Larik, F.A., Hassan, M., Raza, H., and Seo, S.-Y., *Bioorg. Chem*., 2017, vol. 74, p. 187. doi 10.1016/j.bioorg.2017.08.002
30. Campo, R., Criado, J.J., García, E., Hermosa, M.R., Jimenez-Sanchez, A., Manzano, J.L., Monte, E., Rodrıguez-Fernández, E., and Sanz, F., *J. Inorg. Biochem*., 2002, vol. 89, p. 74. doi 10.1016/S0162-0134(01)00408-1
31. Plutín, A.M., Alvarez, A., Mocelo, R., Ramos, R., Castellano, E.E., Silva, M.M., Colina-Vegas, L., Pavan, F.R., and Batista, A.A., *Inorg. Chem. Commun*., 2016, vol. 63, p. 74. doi 10.1016/j.inoche.2015.11.020
32. Chetana, P.R., Srinatha, B.S., Somashekar, M.N., and Policegoudra, R.S., *J. Mol. Struct*., 2016, vol. 1106, p. 352. doi 10.1016/j.molstruc.2015.10.010
33. Larik, F.A., Saeed, A., Fattah, T.A., Muqadar, U., and Channar, P.A., *Appl. Organomet. Chem*., 2016, vol. 31, no. 8, article ID e3664. doi 10.1002/aoc.3664
34. Alvar, J., Yactayo, S., and Bern, C., *Trends Parasitol*., 2006, vol. 22, p. 552. doi 10.1016/j.pt.2006.09.004
35. Antinori, S., Schifanella, L., and Corbellino, M., *Eur. J. Clin. Microbiol*., 2012, vol. 31, p. 109. doi 10.1007/s10096-011-1276-0
36. Chan-Bacab, M.J. and Pena-Rodríguez, L.M., *Nat. Prod. Rep*., 2001, vol. 18, p. 674. doi 10.1039/B100455G
37. Faisal, M., Saeed, A., Shahzad, D., Fattah, T.A., Lal, B., Channar, P.A., Mahar, J., Saeed, S., Mahesar, P.A., and Larik, F.A., *Eur. J. Med. Chem*., 2017, vol. 141, p. 386. doi 10.1016/j.ejmech.2017.10.009
38. Cars, O., Hedin, A., and Heddini, A., *Drug Resist. Updates*, 2011, vol. 14, p. 68. doi.org/10.1016/j.drup.2011.02.006
39. Lai, C.C., Lee, K., Xiao, Y., Ahmad, N., Veeraraghavan, B., Thamlikitkul, V., Tambyah, P.A., Nelwan, R., Shibl, A.M., Wu, J.J., Seto, W.H., and Hsueh, P.R., *J. Global Antimicrob. Resist*., 2014, vol. 2, p. 141. doi 10.1016/j.jgar.2014.02.007
40. Woodford, N. and Ellington, M.J., *Clin. Microbiol. Infect*., 2007, vol. 13, p. 5. doi 10.1111/j.1469-0691.2006.01492.x
41. Freire-Moran, L., Aronsson, B., Manz, C., Gyssens, I.C., So, A.D., Monnet, D.L., and Cars, O., *Drug Resist. Updates*, 2011, vol. 14, p. 118. doi 10.1016/j.drup.2011.02.003
42. Alvan, G., Edlund, C., and Heddini, A., *Drug Resist. Updates*, 2011, vol. 14, p. 70. doi 10.1016/j.drup.2011.01.007
43. Wise, R., *J. Antimicrob. Chemother*., 2011, vol. 66, p. 1939. doi 10.1093/jac/dkr261
44. Saeed, A., Haroon, M., Muhammad, F., Larik, F.A., Hesham, E.S., and Channar, P.A., *J. Organomet. Chem*., 2017, vol. 834, p. 88.
45. Saeed, S., Rashid, N., Jones, P.G., Ali, M., and Hussain, R., *Eur. J. Med. Chem*., 2010, vol. 45, p. 1323. doi 10.1016/j.ejmech.2009.12.016
46. Saeed, A., Khurshid, A., Bolte, M., Fantoni, A.C., and Erben, M.F., *Spectrochim. Acta, Part A*, 2015, vol. 143, p. 59. doi 10.1016/j.saa.2015.02.042
47. Saeed, A., Shaheen, U., Hameed, A., and Naqvi, S.Z.H., *J. Fluorine Chem*., 2009, vol. 130, p. 1028. doi 10.1016/j.jfluchem.2009.09.003
48. Mehfooz, H., Saeed, A., Sharma, A., Albericio, F., Larik, F.A., Jabeen, F., Channar, P.A., and Flörke, U., *Crystals*, 2017, vol. 7 p. 211. doi 10.3390/cryst7070211
49. Halgren, T.A., *J. Comput. Chem*., 1996, vol. 17, p. 587. doi 10.1002/(SICI)1096-987X(199604)17:5/6<520::AID-JCC2>3.0.CO,2-W
50. Abdul Fattah, T., Saeed, A., Channar, P.A., Ashraf, Z., Abbas, Q., Hassan, M., and Larik, F.A., *Chem. Biol. Drug Des*., 2018, vol. 91, p. 434. doi 10.1111/cbdd.13090
51. Schlagenhauf, E, Etges, R., and Metcalf, P., *Structure*, 1998, vol. 6, p. 1035. doi 10.1016/S0969-2126(98)00104-X
52. Isnard, A., Shio, M.T., and Martin, O., *Front. Cell. Infect. Microbiol*., 2012, vol. 2, p. 72. doi 10.3389/fcimb.2012.00072
53. Vicens, Q. and Westhof, E., *Structure*, 2001, vol. 9, p. 647. doi 10.1016/S0969-2126(01)00629-3
54. Saeed, A., Khurshid, A., Jasinski, J.P., Pozzi, C.G., Fantoni, A.C., and Erben, M.F., *Chem. Phys*., 2014, vol. 431, p. 39. doi 10.1016/j.chemphys.2014.01.009